

Performance of Large Scale Non-equilibrium Plasma MHD Generator Coupled with Radio-Frequency Electromagnetic Field

Guofeng Lou* Non-member

Takayasu Fujino** Member

Yoshihiro Okuno* Member

R-z two-dimensional numerical simulations have been carried out to investigate the performance of a large-scale disk MHD generator coupled with radio-frequency (rf) electromagnetic field. The rf technique is verified to be useful even for a large scale MHD generator. The skin effect of plasma influences the distribution of rf electric field, however under the present plasma condition in the MHD generator, this effect will not induce the failure of rf application. When the plasma does not achieve the fully ionized seed condition only by self-induced Joule heating, the plasma is unstable. Coupling with the rf power can stabilize the plasma and improve the performance of generator. Thus, the present rf technique can help widening the actual operating condition of MHD generator.

Keywords: MHD generator, non-equilibrium plasma, rf electromagnetic field, skin effect

1. Introduction

A closed cycle MHD generator uses an alkali-metal seeded noble gas as the working gas. A non-equilibrium plasma is usually produced and self-sustained by Joule heating in the MHD generator⁽¹⁾. The self-sustained plasma makes a system simple, however, it sometimes causes the difficulties of keeping plasma in a suitable condition and matching internal impedance of generator with a load resistance. In a disk shaped MHD generator, the plasma can be produced in the nozzle. To achieve a high performance, the working gas (seed material) should be ionized at the channel inlet with a relatively high electron temperature and the plasma should satisfy the fully ionized seed condition in the channel. The variation of operating condition can cause the plasma to depart from the fully ionized seed condition. When the inlet electron temperature is not high enough or the load resistance is much lower, the joule heating in the MHD channel cannot supply enough energy to sustain the fully ionized seed plasma. This will cause an instability of plasma and deteriorate the performance. Then, the external energy sources can be utilized to produce or sustain the suitable plasma in the generator.

Radio-frequency (rf) electromagnetic field, which is widely used in material process, sinter and analytical chemistry, has been suggested to pre-ionize the working gas and improve the performance of the MHD generator⁽²⁾. Experimental and numerical researches on coupling rf power to MHD generator have been carried out

at Tokyo Institute of Technology. The experiment with a shock tube driven disk MHD generator demonstrated a significant improvement of performance by applying the rf power⁽³⁾. With r- θ two dimensional numerical simulations, the operating conditions, where coupling rf power can improve the performance of MHD generator, have been examined⁽²⁾⁽⁴⁾.

However, these researches were based on relatively small disk MHD generators with the thermal inputs from several to ten mega watts. For large scale MHD generator, on the other hand, the volume of plasma between the rf coils is very large comparing with the smaller MHD generator. Because of the skin effect of plasma, whether the rf electromagnetic field can effectively influence the plasma at the center of large size channel, and what kind of effect will take place when the rf technique is applied to large scale generator, should be clarified. In the present work, r-z two dimensional numerical simulations have been carried out to investigate the effect of rf power on the performance of a large scale disk MHD generator, of which the thermal input is about 100 MWt.

2. Numerical Procedure

2.1 Generator and Operating Conditions

The schematic diagram of the disk MHD generator and the position of rf coils are shown in Fig. 1. The right hand cylindrical coordinates system is adopted. The working gas flows along the r-direction and the magnetic field is applied in the z-direction. The MHD channel covers the area from the upstream edge of anode ($r = 360$ mm) to the downstream edge of cathode ($r = 780$ mm), and between two walls in the z-direction. The heights at inlet and outlet are 59.9 mm and 79.9 mm, respectively. Two ring shape rf coils are used in the present research. The distance from the coil to the wall

* Department of Energy Sciences, Tokyo Institute of Technology
4259, Nagatsuta, Midori-ku, Yokohama 226-8502

** Institute of Engineering Mechanics and Systems, University of Tsukuba
1-1-1, Tennoudai, Tsukuba, Ibaraki 305-8573

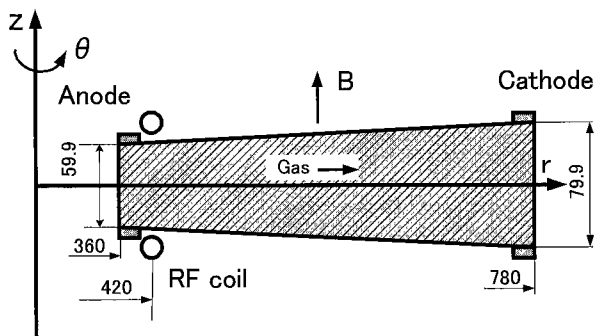


Fig. 1. Schematic of disk MHD generator

Table 1. The operating conditions

Working gas	He-Cs
Inlet stagnation temperature	2000 [K]
Inlet stagnation pressure	3.0 [atm]
Magnetic flux density	6.0 [T]
Inlet Mach number	2.2
Thermal input	117 [MW]
Seed fraction	1.0-3.0x10 ⁻⁵
Load resistance	1.0-9.0 [Ω]
Frequency of rf power	13.56 [MHz]

is 4 mm at $r = 420$ mm. Table 1 shows the operating conditions for the present numerical simulation.

2.2 Governing Equations of rf Electro-magnetic Field Based on the Maxwell's equations and generalized Ohm's Law, using the vector potential \mathbf{A} , the governing equations of rf electromagnetic field can be written out,

$$\nabla^2 \mathbf{A} = \mu_0 \frac{\sigma}{1 + \beta^2} \frac{\partial \mathbf{A}}{\partial t}, \quad (1)$$

where μ_0 is the permeability, σ the electrical conductivity and β the Hall parameter. Using the sinusoidal model, $\mathbf{A} = (0, A_\theta e^{i\omega t}, 0)$, here $\omega = 2\pi f$ and $i = \sqrt{-1}$, the Eq.(1) can be rewritten as follows,

$$\nabla^2 A_\theta - i\mu_0 \frac{\sigma}{1 + \beta^2} \omega A_\theta = 0. \quad (2)$$

For the numerical solution of Eq.(2), the vector component A_θ can be divided into the real part A_R and the imaginary part A_I , so the Eq.(2) can be rewritten in the r - z two dimensional cylindrical coordinates as follows ^{(2) (5)},

$$\left. \begin{aligned} \frac{1}{r} \frac{\partial}{\partial r} \left(r \frac{\partial A_R}{\partial r} \right) + \frac{\partial^2 A_R}{\partial z^2} - \frac{1}{r^2} A_R + \frac{\mu_0 \sigma \omega A_I}{1 + \beta^2} &= 0, \\ \frac{1}{r} \frac{\partial}{\partial r} \left(r \frac{\partial A_I}{\partial r} \right) + \frac{\partial^2 A_I}{\partial z^2} - \frac{1}{r^2} A_I - \frac{\mu_0 \sigma \omega A_R}{1 + \beta^2} &= 0, \\ A_\theta &= A_R + iA_I. \end{aligned} \right\} \quad (3)$$

Induced rf electric field E_θ can be reduced as follows,

$$E_\theta = -i\omega A_\theta. \quad (4)$$

2.3 Governing Equations of MHD Plasma Flow

Based on the engineering conditions, charge-neutrality and low magnetic Reynolds number assumptions are hired. A simple two-temperature model is adopted for non-equilibrium plasma. So the governing equations of MHD plasma flow are written as follows.

(1) Governing equations of heavy particles Continuity equation

$$\frac{\partial \rho}{\partial t} + \nabla \cdot (\rho \mathbf{u}) = 0, \quad (5)$$

where ρ is the mass density and \mathbf{u} is the velocity. Momentum equation

$$\frac{\partial(\rho \mathbf{u})}{\partial t} + \nabla \cdot (\rho \mathbf{u} \mathbf{u}) = -\nabla P + \nabla \cdot \tau_{ij} + \mathbf{j} \times \mathbf{B}, \quad (6)$$

where P is the static gas pressure and τ_{ij} is the viscous stress tensor.

Energy equation

$$\begin{aligned} \rho \left[\frac{\partial(C_v T)}{\partial t} + \mathbf{u} \cdot \nabla(C_v T) \right] \\ = -p \nabla \cdot \mathbf{u} + \Phi + \nabla \cdot (k \nabla T) + \frac{|j|^2}{\sigma} + \frac{\sigma}{1 + \beta^2} \frac{|E_\theta|^2}{2}, \end{aligned} \quad (7)$$

where T is the static gas temperature, c_v the specific heat at constant volume, Φ the dissipation function. and k the coefficient of thermal conductivity.

(2) Governing equations of charged particles Continuity equation

$$\left. \begin{aligned} \frac{\partial n_i^+}{\partial t} + \nabla \cdot (n_i^+ \mathbf{u}) &= \dot{n}_i^+ = k_{fi} n_e n_i - k_{ri} n_e^2 n_i^+, \\ n_e &= \sum_i n_i^+, \end{aligned} \right\} \quad (8)$$

where n_i^+ is the number density of i th particle ions, \dot{n}_i^+ the production rate of i th particle ions, n_e the electron number density, n_i the number density of i th particle atoms, k_{fi} and k_{ri} are the ionization and recombination rate coefficients of i th particle, respectively.

Generalized Ohm's law

$$\mathbf{j} + \frac{\beta}{|\mathbf{B}|} \mathbf{j} \times \mathbf{B} = \sigma(\mathbf{E} + \mathbf{u} \times \mathbf{B}), \quad (9)$$

where \mathbf{j} is the current density, \mathbf{E} the electric field strength, \mathbf{B} the magnetic flux density.

Electron energy equation

$$\begin{aligned} \frac{|j|^2}{\sigma} + \frac{\sigma}{1 + \beta^2} \frac{|E_\theta|^2}{2} &= 3n_e m_e k(T_e - T) \sum_h \frac{v_{eh}}{m_h} \\ &+ \sum_i \dot{n}_i^+ \left(\frac{3}{2} kT_e + \varepsilon_i \right), \end{aligned} \quad (10)$$

$$(h = \text{Seed, Noble Gas, Ion})$$

$$(i = \text{Seed, Noble Gas})$$

where k is the Boltzman constant, T_e the electron temperature, ν_{eh} the collision frequency for electrons with h th particle, m_h the mass of h th particle, and ε_i the ionization energy of i th particle.

Maxwell equations

$$\left. \begin{aligned} \nabla \times \vec{E} &= 0, \\ \nabla \cdot \vec{j} &= 0. \end{aligned} \right\} \dots\dots\dots (11)$$

Perfect gas status equation

$$p = \rho RT. \dots\dots\dots (12)$$

The rf electromagnetic field influences the MHD plasma through an additional Joule heating that is caused by the rf electric field induced in the plasma. This effect is described in the energy equations of heavy particles and electrons. The induced electric field also exerts Lorentz force on MHD plasma flow, which includes two parts. One is $(1/2\rho)[(\sigma/(1+\beta^2))\mathbf{E}_{rf} \times \mathbf{B}_{rf}]$ that is caused by the induced current in the rf magnetic field. The other is caused by the induced current in the steady magnetic field. The former is very small comparing with the term $(1/\rho)(\mathbf{j} \times \mathbf{B})$, so it can be neglected⁽⁶⁾. The second part of the force changes the direction with a frequency of rf electromagnetic field, so in the actual simulation, during the plasma flow in one mesh distance, this force changes the direction several ten times. With this reason the total effect of this force is neglected in the present research. Thus, the Lorentz force caused by rf electric field is not included in the momentum Eq. (6).

Because the electrodes shown in Fig.1 can be segmented in the azimuthal direction, the inductive current is assumed not to flow in the electrode. Moreover the possible effect of the current induced in a casing of MHD generator facility is not taken into account.

2.4 Numerical Method In the calculation region shown in Fig.1, the mesh number is 105 in r -direction and is 40 in z -direction. The time step is $0.05 \mu\text{s}$. SOR method⁽⁶⁾ is used to solve the Poisson Eq. (3) of the rf electromagnetic field. Because the value of vector potential at each point depends on all of the current-carrying regions, the vector potential on the boundary is determined by the superposition of the coil and plasma effects. In the numerical integration, the plasma in the disk MHD generator is divided into a number of control volume elements in form of cylindrical loops, so the boundary condition can be pre-calculated by the following equations for solving the Poisson equations⁽⁷⁾:

$$A_R(R_{bc}, Z_{bc})$$

$$= \frac{\mu_0}{2\pi} \sqrt{\frac{R_c}{R_{bc}}} \sum_{i=1}^{N_{coil}} I_{ci} G(k_i)$$

$$+ \frac{\mu_0 \omega}{2\pi} \sum_{j=1}^{N_{element}} \sqrt{\frac{r_j}{R_{bc}}} \frac{\sigma_j}{1+\beta_j^2} A_{Ij} S_j G(k_j),$$

$$\dots\dots\dots (13)$$

$$A_I(R_{bc}, Z_{bc})$$

$$= -\frac{\mu_0 \omega}{2\pi} \sum_{j=1}^{N_{element}} \sqrt{\frac{r_j}{R_{bc}}} \frac{\sigma_j}{1+\beta_j^2} A_{Rj} S_j G(k_j),$$

$$\dots\dots\dots (14)$$

where the summation of i is for the number of rf coils, and the summation of j is for the number of control volume elements. R_{bc} and Z_{bc} are the radius and height of boundary point, respectively. R_c is the radius of rf coil, I_{ci} is the current in rf coils. A_{Rj} and A_{Ij} are the real and the imaginary part of vector potential of the j th control volume element. r_j and S_j are the radius and the cross section of the j th control volume element. Here,

$$G(k) = \frac{(2-k^2)K(k) - 2E(k)}{k}, \dots\dots\dots (15)$$

$$k^2 = \frac{4R_c r}{(R_c + r)^2 + (Z - Z_c)^2}. \dots\dots\dots (16)$$

In the above equation, K and E are the complete elliptic integrals of the first and second kinds, respectively. Z_c is the height of rf coil.

Hyperbolic Eqs. (5), (6), (7) and (8) are solved by CIP method⁽⁸⁾. From the general Ohm's law (9) and Maxwell equations (11), a scalar potential function two-order elliptic equation can be obtained and is solved by the finite difference method. For the supersonic flow, the inlet parameters are given as inlet boundary conditions. The outlet boundary is decided by free boundary condition. No-slip boundary condition is used for walls, and the wall temperature is given. For the elliptic equation the boundary conditions are calculated for every boundary surface. The detail description can be found in Ref. (9).

3. Results and Discussion

3.1 Inlet Electron Temperature with rf Electric Field and rf Joule Heating in MHD Plasma

The inlet electron temperature in the presence of rf electromagnetic field depends on the intensity of rf electric field at the inlet boundary. The inlet electron temperature under a operating condition (seed fraction = 1.0×10^{-5} , $RL = 2.0 \Omega$) is drawn as a function of current in rf coil in Fig. 2(a). It is shown that the inlet temperature increases with the rf coil current. In the present research, all of the inlet electron temperature with rf electric field is determined by this way. The ratio of Joule heating caused by rf electric field in MHD plasma depending on the current in rf coil is shown in Fig. 2(b). Although the rf power can significantly increase the performance of MHD generator, which is described in the following sections, the cost of rf energy is not more than 0.8% of the thermal input for the operating condition. When the current is 190 A as a typical value, it is only about 0.16%.

3.2 rf Electric Field in MHD Plasma When the plasma is exposed to the rf electromagnetic field that has a frequency below the electron plasma frequency, the interaction of the rf energy with the plasma occurs in the

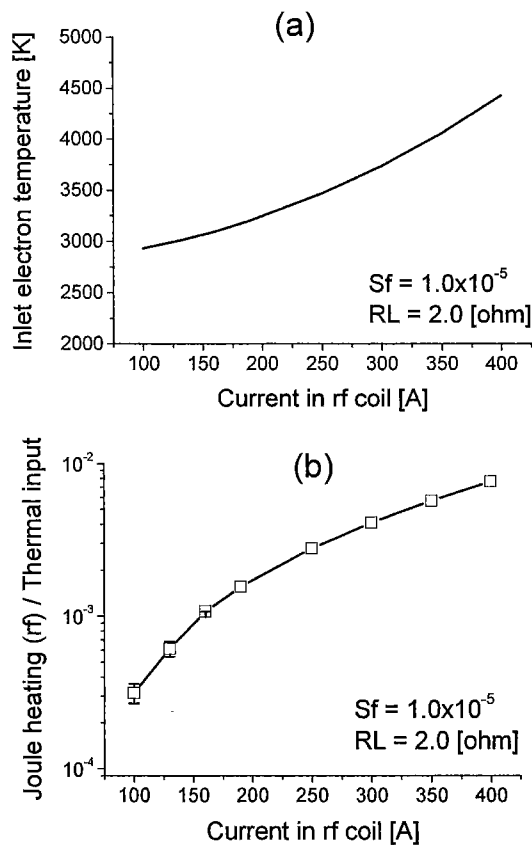


Fig. 2. (a) Inlet electron temperature and (b) ratio of Joule heating of rf electric field to thermal input as a function of current in rf coil

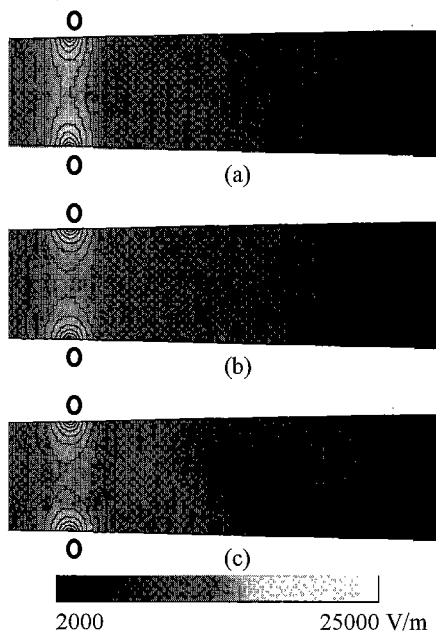


Fig. 3. Distribution of rf electric field in r-z plane ($I_c = 190$ A, $RL = 2.0$ Ω). (a) not including the skin effect, (b) including the skin effect ($Sf = 1.0 \times 10^{-5}$), (c) including the skin effect ($Sf = 2.5 \times 10^{-5}$)

skin depth. The interaction makes the rf electric field in MHD plasma modified from that in free space. Figure 3 shows the r-z plane distribution of rf electric field in MHD channel. The case (a) does not include the skin

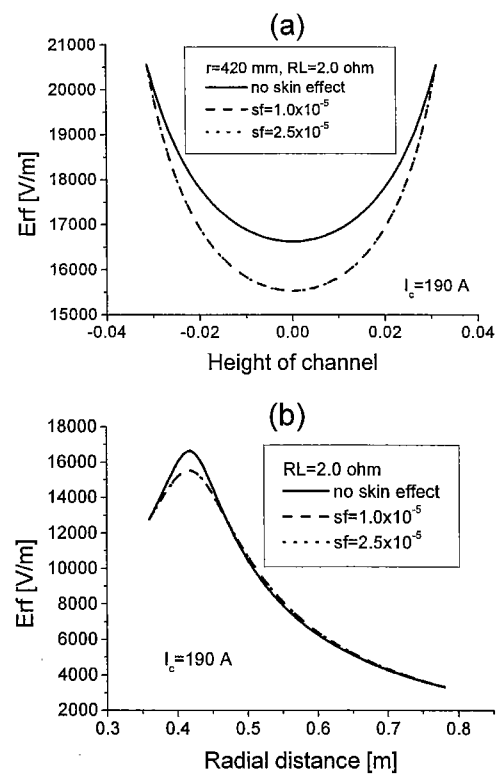


Fig. 4. Distribution of rf electric field, (a) along the height of channel, (b) along r-direction in the center of channel

effect in MHD plasma (as in free space). The case (b) and (c) are the distributions that include the skin effect. The distributions of rf electric field along the height of channel at the position ($r = 420$ mm) where the rf coils are located, and the distribution along the fluid flow in the center of channel are drawn in Figs. 4(a) and (b), respectively. It can be found from Fig. 4(a) that the skin effect decreases the rf electric field in the plasma. The difference between the rf electric fields with the skin effect and without it becomes the biggest at the center. Along the fluid flow the biggest difference is found at the position of rf coils ($r = 420$ mm). The difference decreases with the increase of distance from rf coils, and for the distance larger than 50 mm it varies little. Consequently, the interaction between MHD plasma and rf electromagnetic field decreases the rf electric field near the rf coils, however the distribution of rf electric field is hardly affected at the location far away. The distributions of rf electric field for different plasma conditions in Fig. 3 and Fig. 4, which include the skin effect, are very similar. It means that the variation of plasma condition in the present research causes little difference in the rf electric field.

3.3 Effect of rf Power on Performance of MHD Generator with Different Load Resistance The enthalpy extraction ratio and the isentropic efficiency are important efficiencies to describe the performance of MHD generator. Keeping the seed fraction constant (1.0×10^{-5}), the enthalpy extraction ratios when coupled with rf power or not are drawn as a function of load resistance in Fig. 5(a), and the isentropic efficiency

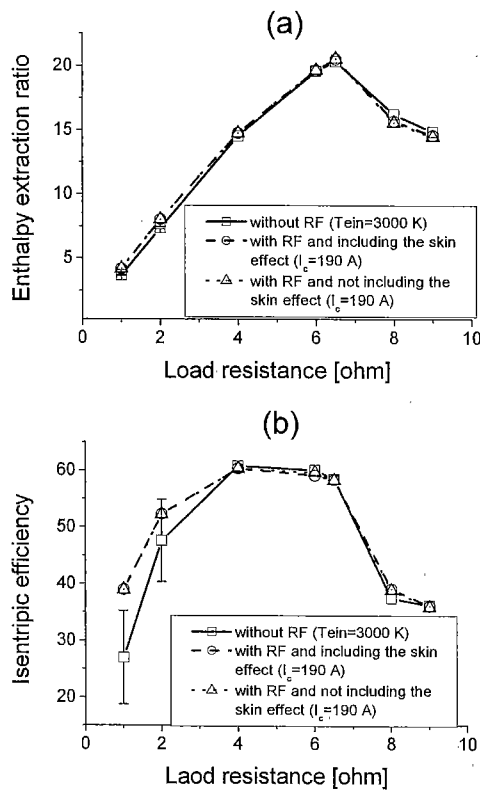


Fig. 5. Enthalpy extraction ratio and isentropic efficiency versus load resistance

in Fig. 5(b). The current in rf coil is 190 A for coupling rf power, which is a lower limit for effective use of rf power. The inlet electron temperature is assumed as 3000 K when no rf power is coupled to MHD generator. In Fig. 5(a), when the load resistance is low, applying rf power increases the enthalpy extraction ratio, on the contrary, for high load resistance the situation is inverse, although both of the increase and the decrease are small. When the load resistance is about 6.5Ω that corresponds to highest efficiency, applying rf power has little effect on the performance of generator. Figure 5(b) shows that applying rf power can increase the isentropic efficiency largely for small load resistance, however for high load resistance it has little effect. For a relatively lower inlet electron temperature and a small load resistance, the plasma is unstable, however the coupling rf power can stabilize the plasma, then improve the performance of MHD generator. Unlike that of load resistance being lower, when the load resistance is high, the Joule heating can support enough energy to ionize the seed, so the seed is fully ionized in the channel no matter whether coupling with rf power or not. It means that the plasma is stable for both operating conditions. For high seed fraction (2.5×10^{-5}), as will be discussed in the next section, coupling with rf power can help achieving the high performance. However, even in that case, the effect of coupling rf power becomes small with the increase of the load resistance. Generally, coupling with rf power has little effect on performance of MHD generator with high load resistance.

Furthermore, it is found from Fig. 5 that the

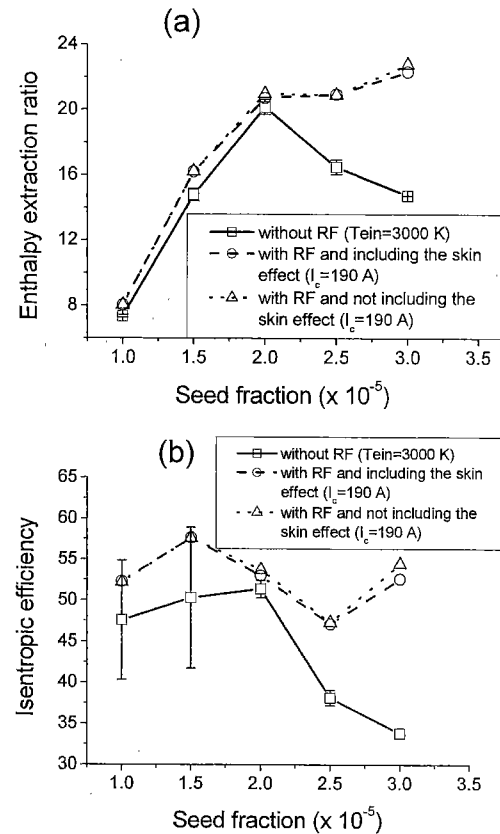


Fig. 6. Enthalpy extraction ratio and isentropic efficiency versus seed fraction (RL=2.0 Ω)

performance of MHD generator is almost the same with including the skin effect or not. It implies that although the distributions of rf electric field are affected by the skin effect, both of them can supply the enough energy to stabilize the MHD plasma by fully ionizing the seed.

3.4 Effect of rf Power on Performance of MHD Generator with Different Seed Fraction

For a constant load resistance of 2Ω , the efficiencies versus seed fraction are drawn in Fig. 6. In Fig. 6(a), the enthalpy extraction ratio has a small fluctuation for not coupling with rf power. With coupling with rf power, the fluctuation is reduced completely and the enthalpy extraction ratio increases, especially for seed fraction being high. It can be found from Fig. 6(b) that without coupling rf power the isentropic efficiency fluctuates and for low seed fraction the fluctuation is very large (about 30% of the mean value). With coupling rf power, not only the fluctuation is depressed but also the isentropic efficiency increases. To contrast the structures of plasma with coupling rf power or not, the distributions of electron temperature in the r - z plane are drawn in Fig. 7. It can be seen that the plasma is unstable if not coupling rf power, and with coupling rf power the plasma becomes stable. The self-sustained Joule heating is not able to supply enough energy to ionize the seed when the rf power is not applied, so the instability of MHD plasma occurs. Under this condition, coupling rf power can help achieving the fully ionized seed plasma, stabilizing the plasma, and increasing the effective electrical conductivity. These can increase the efficiency of MHD

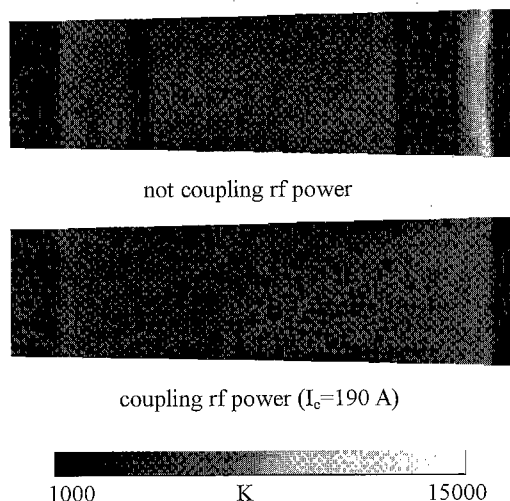


Fig. 7. Distribution of electron temperature in r-z plane ($RL=2\ \Omega$, $sf=2.5\times 10^{-5}$)

generator. Thus, the technique of coupling rf power allows that the wide operating condition is available in the actual operation of MHD generator, although the effect of the coupling rf power becomes small with the decrease of the seed fraction for high load resistance, as can be understood with the argument in the previous section.

Finally a brief comment for more large scale MHD generator is added. The inlet height of generator with a thermal input of about 1000 MWt can be several ten centimeters (20~30 cm). In that case, the frequency of rf power should be lowered (~several MHz). The present rf technique is expected to be useful even for more large MHD generator, although the simulation has not been carried out because of the ability of present computers.

4. Conclusions

The performance of a large-scale disk MHD generator coupled with an rf power has been investigated with r-z two-dimensional numerical simulations. The main conclusions are summarized as follows:

(1) The rf technique is useful even for a large scale MHD generator. The skin effect of plasma influences the distribution of rf electric field, however under the present plasma condition of MHD generator; this effect will not induce the failure of rf application. Thus, the present rf technique can help widening the actual operating condition of MHD generator.

(2) For the low load resistance, the plasma is unstable. Applying rf power to the generator can make plasma stable and improve the performance. On the other hand, coupling rf power has little effect on the performance for a relatively high load resistance.

(3) When seed fraction is high, self-sustained Joule heating is not able to supply enough energy to ionize the whole of seed. This induces the instability of plasma. Coupling rf power can effectively stabilize the plasma and improve the performance.

(Manuscript received April 25, 2003,

revised July 29, 2003)

References

- (1) R.J. Rosa: *Magnetohydrodynamic Energy Conversion*, McGraw-Hill, New York (1968)
- (2) T. Murakami, Y. Okuno, and S. Kabashima: "Plasma Stabilization and Improvement in the performance of a Nonequilibrium Disk MHD Generator by a Radio-Frequency Electromagnetic field", *IEEE Trans. Plasma Sci.*, Vol.27, No.2, pp.604-612 (1999-4)
- (3) T. Fujino, T. Murakami, Y. Okuno, and H. Yamasaki: "Experiments of Non-Equilibrium MHD Power Generation with Radio-Frequency Pre-ionization", *Proceedings of the 14th International Conference on MHD Electrical Power Generation and High Temperature Technologies*, pp.413-420, Hawaii (2002-5)
- (4) J. Enogaki, T. Fujino, T. Murakami, Y. Okuno, and H. Yamasaki: "Plasma and Fluid Behavior in a Disk MHD Generator under Radio-Frequency electromagnetic Field", *Proc. for Symposium on Advance Research of Energy Technology 2002*, pp.103-112, Hokkaido (2002-3)
- (5) R.J. Uncles and A.H. Nelson: "Dynamic stabilization of the electrothermal instability", *Plasma Physics*, Vol.12, pp.917-926 (1970)
- (6) M.N.O. Saiku: *Numerical Techniques in Electromagnetics*, p154, CRC Press (1992)
- (7) T. Suekane, T. Taya, Y. Okuno, and S. Kabashima: "Numerical Studies on the Nonequilibrium Inductively Coupled Plasma with Metal Vapor Ionization", *IEEE Trans. Plasma Sci.*, Vol.24, No.3, pp.1147-1154 (1996-6)
- (8) P.-Y. Wang, T. Yabe, and T. Aoki: "A General Hyperbolic Solver-the CIP Method-Applied to Curvilinear Coordinate", *J. Phy. Soc. Japan*, Vol.62, No.6, pp.1865-1871 (1993)
- (9) H. Kobayashi, Y. Okuno, and S. Kabashima: "Three-Dimensional Structures of MHD Flow in a Disk Generator", *IEEE Trans. Plasma Sci.*, Vol.26, No.5, pp.1526-1531 (1998-10)

Guofeng Lou (Non-member) received the B.E. degree from Beijing University of Sciences and Technology in 1990 and M.E. degree from Institute of Electrical Engineering (IEE), Chinese Academy Sciences (CAS) in 1997. He is presently a doctoral student at Tokyo Institute of Technology. His research interests are the MHD power generation, magnetohydrodynamics and non-equilibrium plasma.



Takayasu Fujino (Member) received the B.S. degree from Science University of Tokyo in 1997, and the M.E. and D.E. degrees in Energy Sciences from Tokyo Institute of Technology, in 1999 and 2002, respectively. He is presently a Research Fellow of the Japan Society for the Promotion of Science. His research interests include the MHD power generation and chemical reactional air plasma.



Yoshihiro Okuno (Member) received the B.E. degree in Electrical Engineering from Kyushu Institute of Technology in 1982 and the M.E. and D.E. degrees in Energy Sciences from Tokyo Institute of Technology in 1984 and 1987, respectively. He is presently a professor at Tokyo Institute of Technology.

